PERGAMON

International Journal of Solids and Structures 36 (1999) 2891–2915

INTERNATIONAL JOURNAL OF SOLIDS and STRUCTURES

A method for the analysis of plates on a two-parameter foundation

Mecit Çelik*, Ahmet Saygun

Faculty of Civil Engineering, Istanbul Technical University, Maslak 80626, Istanbul, Turkey

Received 3 December 1997; in revised form 3 April 1998

Abstract

In this study, an iterative method is developed in order to analyze the plates on a two-parameter elastic foundation, based on the study by Vallabhan et al. (1991), where the material properties of the soil are used in order to compute the coefficients of subgrade reactions, for the layered soil medium. In the analysis, the finite element method is used, both plate and surrounding soil area divided into finite elements. The plate finite element is considered by including the effects of subgrade reactions. By means of the method suggested herein, it is possible to examine the interaction between the separate plates close to each other and to assume the plate of arbitrary shape. © 1999 Elsevier Science Ltd. All rights reserved.

Keywords: Elastic bedding coefficient; Shear parameter coefficient; Mode shape parameter; Plate finite element; Soil finite element

1. Introduction

It is known that the shear parameter effect is used in addition to the Winkler coefficient for the analysis of a one-dimensional beam and two-dimensional foundation plate on a two-parameter elastic foundation. Comparing the similar models (Filonenko-Borodich, Pasternak), the model developed by Vlasov and Leontev has the advantage of determining the soil parameters depending on soil material properties and the thickness of the compressible layer. Karamanlidis and Prakash (1988) gave the stiffness and the mass matrix for beams which have four degrees-of-freedom, on a two-parameter elastic foundation by using cubic Hermitian polynomials as trial functions in shape function. Razaqpur and Shah (1991) derived a new finite element, where the stiffness matrix, the nodal load vector and the shape function of the element are derived by using the differential equation of a beam on a two-parameter foundation. Nogami and O'Neil (1985) suggested that the vertical displacements can be expressed with a series of displacement shapes which are harmonically varying in depth. Nogami and Lam (1987) developed a two-parameter model for slabs on elastic

* Corresponding author. Fax: 00 90 212 2856587; E-mail: mcelik@srv.ins.itu.edu.tr

PII: S0020–7683(98)00135–8

foundations, where the foundation layer is divided into a number of horizontal layers. Here each layer is idealized by a system of multiple one-dimensional vertical columns interconnected by shear springs. The elastic beddings and the shear parameter coefficients are obtained by using elastic constants and the depth of the foundation.

Vallabhan and Das (1988) developed an iterative procedure to obtain a mode shape parameter by minimizing the total potential energy, where the elastic constants of the beam and the mode of loading are used as a function in addition to the thickness of the compressible layer and the elastic constants of the foundation. They also determined the elastic bedding and shear parameter coefficients. Vallabhan and Das (1991) developed a new model, where the elastic properties of the layer vary linearly with depth. Jones and Xenophontos (1977) expressed the elastic bedding and shear parameter coefficients depending on a mode shape parameter, reciprocally a mode shape parameter depending on the displacement shape of the top of the soil. They used variational principles and the mode shape parameter was obtained by experimental investigation instead of an iterative procedure.

Vallabhan et al. (1991) extended their model for the analysis of plates on an elastic foundation as is summarized below.

2. Governing equations and the expressions for plates on an elastic foundation

The lateral displacements in the soil can be assumed to be negligible compared to the displacement in the vertical direction. The displacement in the vertical direction was assumed to be

$$w_z = w(x,y)\phi(z) \tag{1}$$

where $w(x,y)$ is the deflection of the soil surface and $\phi(z)$ is the mode shape function defining the variation of the vertical displacement in the vertical direction, having the boundary condition

$$\phi(z=0) = 1, \quad \phi(z=H) = 0 \tag{2}$$

where H is the thickness of the compressible layer supposed to be known. By minimizing the total potential energy function under the variation of $w(x,y)$, the following equation is obtained in the domain of the plate

$$D\Delta\Delta w - 2C_{\mathrm{T}}\Delta w + Cw = q \tag{3}$$

and outside the domain of the plate

$$-2C_{\mathrm{T}}\Delta w + Cw = 0 \tag{4}$$

where D is the flexural rigidity of the plate $[D = (E_{\mathrm{b}}h^3/12(1-v^2))]$, q is the external load on the plate. By minimizing the total potential energy function by $\phi(z)$ in the domain of the soil $(0 < z < H)$, the function $\phi(z)$ can be expressed as

$$\phi(z) = \frac{\sinh\left[\gamma(1-z/H)\right]}{\sinh\gamma} \tag{5}$$

where γ denotes the mode shape parameter. The elastic bedding coefficient C and the shear parameter coefficient $2C_{\mathrm{T}}$ can be obtained as follows, depending on the mode shape parameter γ:

$$C = \frac{E_s(1-\nu_s)}{(1+\nu_s)(1-2\nu_s)}\frac{\gamma}{H}\frac{[\sinh 2\gamma + 2\gamma]}{4\sinh^2\gamma} \tag{6}$$

$$2C_T = G_s\frac{H}{\gamma}\frac{[\sinh 2\gamma - 2\gamma]}{4\sinh^2\gamma} \tag{7}$$

where E_s, ν_s, G_s are the elastic constants of the soil. The mode shape parameter γ yields as follows:

$$\gamma^2 = H^2\frac{(1-2\nu_s)}{2(1-\nu_s)}\frac{\displaystyle\int_{-\infty}^{\infty}\int_{-\infty}^{\infty}\left\{\left(\frac{\partial w(x,y)}{\partial x}\right)^2 + \left(\frac{\partial w(x,y)}{\partial y}\right)^2\right\}\mathrm{d}x\,\mathrm{d}y}{\displaystyle\int_{-\infty}^{\infty}\int_{-\infty}^{\infty} w^2(x,y)\,\mathrm{d}x\,\mathrm{d}y} \tag{8}$$

As it can be seen in these expressions C and $2C_T$ depend on the material properties, the thickness of the compressible layer of the soil and the coefficient γ. On the other hand, γ depends on the deflection shape of the system, subjected to the external loads. It can be evaluated after determining $w(x, y)$ which satisfies eqn (3) inside the domain of the plate and eqn (4) outside the domain of the plate. It is obvious, that for computing the parameter γ the iterative method has to be used in which γ is initially set, for example equal to unity and it is also used in the computations of the coefficients of subgrade reaction C and $2C_T$. Thus, the deformed shape of the foundation can be obtained. Then, γ is calculated using eqn (8) and the procedure is repeated until the difference between the two successive values of γ will be less than a small prescribed value. In this study it is observed that the iteration process converges more rapidly for uniformly distributed load cases (e.g. 5–6 steps) compared to the concentrated load cases (e.g. 10–12 steps).

Vallabhan et al. (1991) considered in a similar way to that of Vlasov and Leont'ev (1966), the reactions of the foundation along the edge of the plate by using a simplified assumption and by defining equivalent springs along the boundary of the rectangular plate. Vallabhan and Das (1991) also extended their model for the analysis of axisymmetric circular tank foundations. Vallabhan and Daloğlu (1997) employed the finite element method, instead of the finite difference method. Four-noded rectangular finite elements with 12 degrees-of-freedom are developed to model the slab and the soil along with four degrees-of-freedom elements for the beams that stiffen the slab. The stiffness coefficients representing the effects of the infinite soil continuum outside the domain of the soil are determined in a similar way to that of Vallabhan et al. (1991). When the plate does not have a simple rectangular shape or when it has holes, the soil reactions along the inside and the concave edges have to be taken into account by different equivalent spring formulations (Fig. 1).

In this study, the deflections of the soil surface around the plate are considered as well as those under the plate. The deflections of the surface around the plate are obtained by dividing this area into soil finite elements of two dimensions. However, as it is shown by the first author (Çelik, 1996) for practical purposes, it is quite enough to consider a limited soil region around the periphery of the plate, instead of the whole soil surface extending to infinity. It appears from the evaluated examples that the extent of this region can be as the thickness of the compressible layer H of the soil (Fig. 2(b)). Thus, the vertical displacement at the edge of the soil surface can be obtained up to the accuracy of 2–3% along the edge of the plate. The interaction effects between

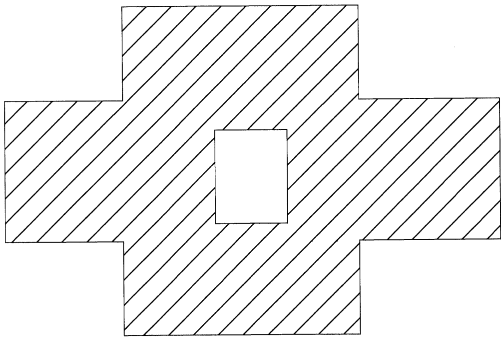

Fig. 1. Plates on the foundation.

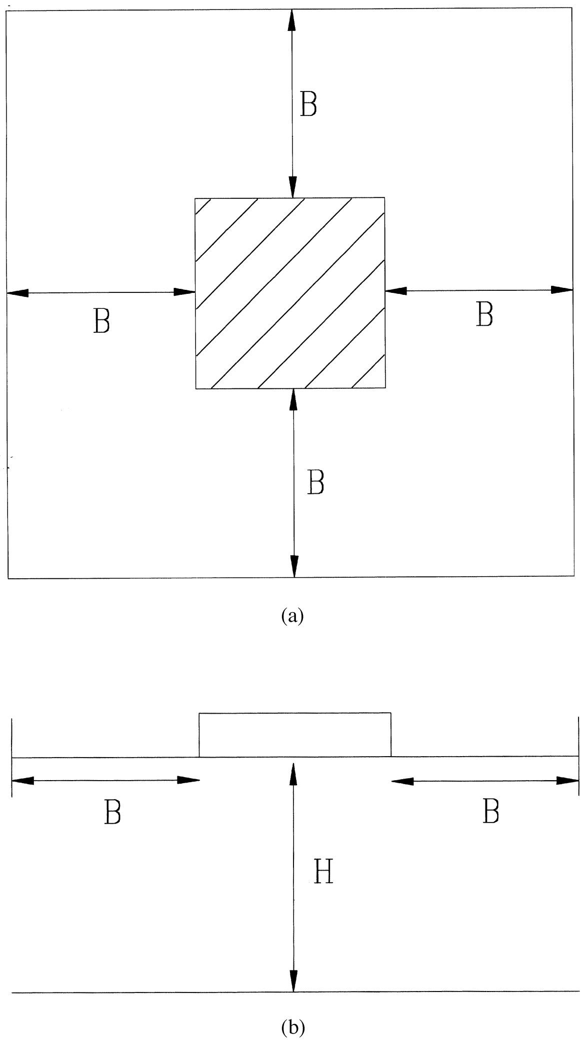

Fig. 2. (a) The plates, (b) the surrounding soil.

the separate plates close to each other can also be analyzed easily, by using the considered finite element idealization.

3. Plate finite elements including the effects of a two-parameter soil

It is known that the distributed soil reaction, which depends on the displacements of soil surface, is expressed as

$$q_z = Cw - 2C_{\mathrm{T}}\left(\frac{\partial^2 w}{\partial x^2} + \frac{\partial^2 w}{\partial y^2}\right) \tag{9}$$

The shear forces along the boundaries depend on the vertical slope ($\partial w/\partial n$) and they are proportional to the shear parameter as shown in Fig. 3.

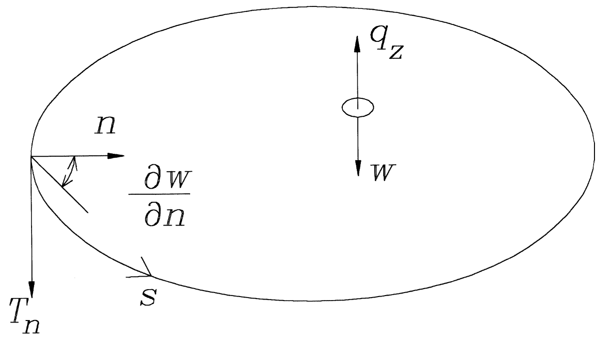

Fig. 3. Soil reactions.

$$T_n = -2C_{\mathrm{T}}\left(\frac{\partial w}{\partial n}\right) \tag{10}$$

As it is well-known, in the finite element method, the displacement shape of an element can be expressed depending on nodal freedom of the element as follows:

$$w(x,y) = \sum_{i=1}^{n} w_i(x,y)d_i \tag{11}$$

and every equivalent nodal force of distributed loads can be calculated as the total work done by the distributed loads with the corresponding unit displacement shape. Each equivalent nodal force of soil reactions can be expressed as:

$$P_{si} = -\iint q_z w_i \,\mathrm{d}A + \oint T_n w_i \,\mathrm{d}s \tag{12}$$

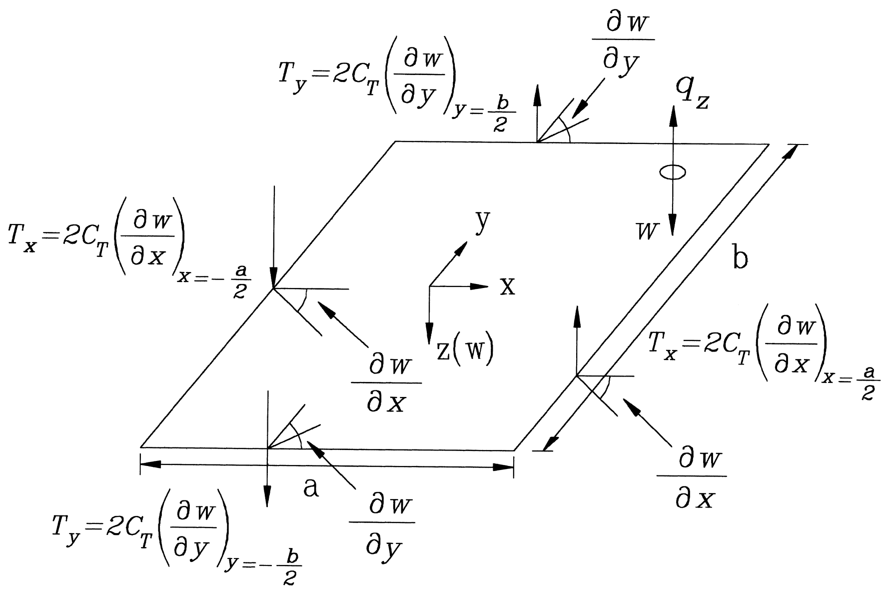

Fig. 4. Soil reactions on a rectangular plate finite element.

Thus, substituting eqn (9) and eqn (10) into eqn (12) the equivalent nodal forces of soil reactions for a rectangular plate element (Fig. 4) are expressed as

$$\begin{aligned}P_{si} = &-C\iint w_i w\,\mathrm{d}A + 2C_\mathrm{T}\iint w_i\left(\frac{\partial^2 w}{\partial x^2}+\frac{\partial^2 w}{\partial y^2}\right)\mathrm{d}A\\ &-2C_\mathrm{T}\int w_i\left(\frac{\partial w}{\partial x}\right)_{x=(a/2)}\mathrm{d}y + 2C_\mathrm{T}\int w_i\left(\frac{\partial w}{\partial x}\right)_{x=-(a/2)}\mathrm{d}y\\ &-2C_\mathrm{T}\int w_i\left(\frac{\partial w}{\partial y}\right)_{y=(b/2)}\mathrm{d}x + 2C_\mathrm{T}\int w_i\left(\frac{\partial w}{\partial y}\right)_{y=-(b/2)}\mathrm{d}x\end{aligned} \tag{13}$$

Partial integration of the second term gives:

$$2C_\mathrm{T}\iint w_i\frac{\partial^2 w}{\partial x^2}\mathrm{d}A = 2C_\mathrm{T}\int\left(w_i\frac{\partial w}{\partial x}\right)_{x=(a/2)}\mathrm{d}x - 2C_\mathrm{T}\int\left(w_i\frac{\partial w}{\partial x}\right)_{x=-(a/2)}\mathrm{d}x - 2C_\mathrm{T}\iint\frac{\partial w_i}{\partial x}\frac{\partial w}{\partial x}\mathrm{d}A \tag{14a}$$

$$2C_\mathrm{T}\iint w_i\frac{\partial^2 w}{\partial y^2}\mathrm{d}A = 2C_\mathrm{T}\int\left(w_i\frac{\partial w}{\partial y}\right)_{y=(b/2)}\mathrm{d}y - 2C_\mathrm{T}\int\left(w_i\frac{\partial w}{\partial y}\right)_{y=-(b/2)} - 2C_\mathrm{T}\iint\frac{\partial w_i}{\partial y}\frac{\partial w}{\partial y}\mathrm{d}A \tag{14b}$$

by rearranging (13)

$$P_{si} = -C\iint w_i w \, \mathrm{d}A - 2C_\mathrm{T}\iint\left(\frac{\partial w_i}{\partial x}\frac{\partial w}{\partial x}+\frac{\partial w_i}{\partial y}\frac{\partial w}{\partial y}\right)\mathrm{d}A \tag{15}$$

is obtained.

Although eqn (15) is obtained for a plate of rectangular shape, it can be generalized for any element shape by using Green's theorem. Substituting eqn (11) into eqn (15) and setting the terms depending on soil reactions on the left side, the equilibrium equation for any nodal freedom of a plate element can be written as follows:

$$\sum_{j=1}^{n} k_{ij}d_j + \sum_{j=1}^{n} C_{ij}d_j + \sum_{j=1}^{n} C_{\mathrm{T}ij}d_j = P_i \tag{16}$$

where

$$C_{ij} = C\iint w_i w_j \, \mathrm{d}A \tag{17}$$

$$C_{\mathrm{T}ij} = 2C_\mathrm{T}\iint\left\{\frac{\partial w_i}{\partial x}\frac{\partial w_j}{\partial x}+\frac{\partial w_i}{\partial y}\frac{\partial w_j}{\partial y}\right\}\mathrm{d}A \tag{18}$$

and k_{ij} and P_i are the standard terms of a stiffness matrix dealing with the flexural rigidity of the plate and the equivalent nodal force due to external loads, respectively.

Equation (16) can be written for the whole freedom of the element in matrix form:

$$[K][d]+[C][d]+[C_\mathrm{T}][d] = [P] \tag{19}$$

4. The elastic bedding [C] and shear parameter [C_T] matrices of rectangular plate elements having 16 and 12 degrees-of-freedom

Using eqns (17) and (18), the term of subgrade reaction matrices [C] and [C_T] of the soil have been computed for Bogner et al. (1966) (for 16 degrees-of-freedom) finite element and Adini and Clough (1961) (for 12 degrees-of-freedom) finite element are given in Appendices 1 and 2.

5. Finite element idealization of a surrounding soil area

As is seen in eqn (4), where no external loads are presented, the behavior of a soil finite element, which will be used for the idealization of the surrounding soil area, can be defined as a shear plate element. It has an elastic bedding coefficient C and a shear rigidity $Gh' = 2C_\mathrm{T}$. A linear variation of the vertical displacement in both directions is assumed for the soil finite element by using the above analogy. Thus, the displacement shape of the soil finite element can be defined as

$$w = \Sigma w_i d_i = [A_\mathrm{d}]_\mathrm{s}[d] \tag{20}$$

where [d] denotes the vertical nodal displacements of the soil finite element and $[A_\mathrm{d}]_\mathrm{s}$ is the shape function of the shear plate element. When the number of soil finite elements increase in the soil medium, the excessive increasing of the nodal parameter can be prevented by choosing only vertical displacement in the soil finite element. The difficulties that may arise from requiring the slope

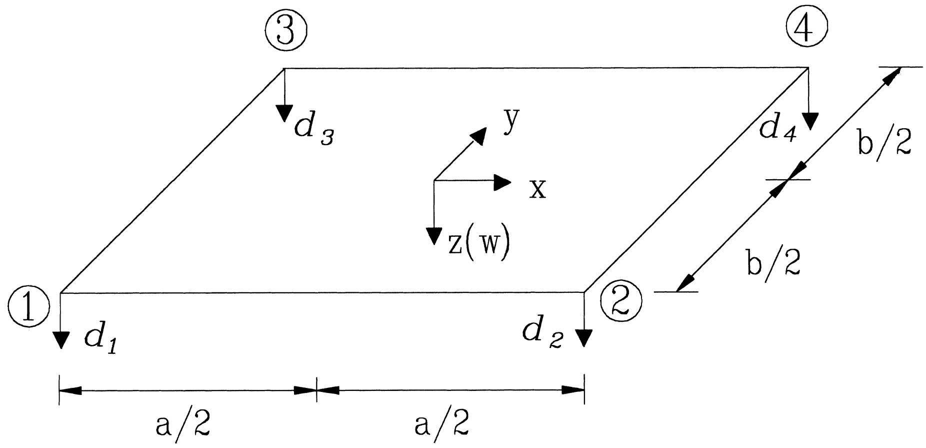

Fig. 5. Rectangular soil finite element.

continuity condition on the edges where the plate finite elements combine with the soil finite elements, are prevented. By using the same procedure adopted for plate elements, the relation between the nodal forces and the displacements of the soil element can be expressed as

$$[C][d]+[C_T][d] = [P] \tag{21}$$

where $[C]$ and $[C_T]$ are the elastic bedding and shear effect matrices of the soil medium. The terms of these matrices can be computed by eqns (17) and (18).

6. Rectangular soil finite element have four degrees-of-freedom

The considered rectangular soil finite element is shown in Fig. 5. The deformed shape can be defined as given in eqns (20) and (22) where $[A_d]_s$ is obtained by multiplying the linear shape function in both directions.

$$[A_d]_s = [l_2(x)l_2(y) \quad l_1(x)l_2(y) \quad l_1(y)l_2(x) \quad l_1(x)l_1(y)] \tag{22}$$

The linear functions are given as:

$$\begin{aligned} l_2(x) &= (0.5-x/a) \quad l_1(x) = (0.5+x/a) \\ l_2(y) &= (0.5-y/b) \quad l_1(y) = (0.5+y/b) \end{aligned} \tag{23}$$

The terms of the elastic bedding and the shear parameter matrix, which are obtained by using eqns (17) and (18), are given in eqns (24) and (25).

$$[C] = \frac{Cab}{36}\begin{bmatrix} 4 & 2 & 2 & 1 \\ 2 & 4 & 1 & 2 \\ 2 & 1 & 4 & 2 \\ 1 & 2 & 2 & 4 \end{bmatrix} \tag{24}$$

$$[C_{\mathrm{T}}] = \frac{2C_{\mathrm{T}}}{3}\begin{bmatrix} \alpha+\beta & \alpha/2-\beta & \beta/2-\alpha & -(\alpha+\beta)/2 \\ \alpha/2-\beta & \alpha+\beta & -(\alpha+\beta)/2 & \beta/2-\alpha \\ \beta/2-\alpha & -(\alpha+\beta)/2 & \alpha+\beta & \alpha/2-\beta \\ -(\alpha+\beta)/2 & \beta/2-\alpha & \alpha/2-\beta & \alpha+\beta \end{bmatrix} \tag{25}$$

where $\alpha = (a/b)$, $\beta = (b/a)$.

By using the stress–displacement relationship, the shear forces within the soil element can be obtained as follows:

$$\begin{bmatrix} T_x \\ T_y \end{bmatrix} = 2C_{\mathrm{T}}\begin{bmatrix} \dfrac{\partial}{\partial x} \\ \dfrac{\partial}{\partial y} \end{bmatrix}[A_{\mathrm{d}}]_{\mathrm{s}}[d] \tag{26}$$

7. Computation of the mode shape parameter (γ)

During the iterative method explained above, the new mode shape parameter γ has to be obtained by using eqn (8), after determining the deformed shape $w(x, y)$ of the system. The integral terms of eqn (8) can be evaluated for every plate and the soil finite element separately. They are extended to the whole system by taking the summation of each element's contribution.

The deformed shape and its partial derivatives with respect to variable x and y within an element can be given as

$$w = \sum_{i=1}^{n} w_i d_i \tag{27}$$

$$\frac{\partial w}{\partial x} + \frac{\partial w}{\partial y} = \sum_{i=1}^{n}\left(\frac{\partial w_i}{\partial x} + \frac{\partial w_i}{\partial y}\right)d_i \tag{28}$$

where the nodal freedoms of the element are known. Hence, the integral terms of an element

$$\iint w^2\,\mathrm{d}A = \iint\left(\sum_{i=1}^{n} w_i d_i\right)\left(\sum_{j=1}^{n} w_j d_j\right)\mathrm{d}A = \sum_{i=1}^{n}\sum_{j=1}^{n}\left(\iint w_i w_j\,\mathrm{d}A\right)d_i d_j \tag{29}$$

$$\iint\left[\left(\frac{\partial w}{\partial x}\right)^2 + \left(\frac{\partial w}{\partial y}\right)^2\right]\mathrm{d}A = \iint\left[\left(\sum_{i=1}^{n}\frac{\partial w_i}{\partial x}d_i\right)\left(\sum_{j=1}^{n}\frac{\partial w_j}{\partial x}d_j\right) + \left(\sum_{i=1}^{n}\frac{\partial w_i}{\partial y}d_i\right)\left(\sum_{j=1}^{n}\frac{\partial w_j}{\partial y}d_j\right)\right]\mathrm{d}A \tag{30}$$

can be calculated using the $[C]$ and $[C_{\mathrm{T}}]$ matrices which are already found.

$$\iint w^2\,\mathrm{d}A = \frac{1}{C}[d]^T[C][d] \tag{31}$$

$$\iint\left[\left(\frac{\partial w}{\partial x}\right)^2+\left(\frac{\partial w}{\partial y}\right)^2\right]\mathrm{d}A = \frac{1}{2C_t}[d]^T[C_T][d] \tag{32}$$

The effects of all the other elements can be summed up for the whole system, as follows:

$$\int_{-\infty}^{\infty}\int_{-\infty}^{\infty} w^2\,\mathrm{d}x\,\mathrm{d}y = \sum_{el}\frac{1}{C}[d]^T[C][d] \tag{33}$$

$$\int_{-\infty}^{\infty}\int_{-\infty}^{\infty}\left[\left(\frac{\partial w}{\partial x}\right)^2+\left(\frac{\partial w}{\partial y}\right)^2\right]\mathrm{d}x\,\mathrm{d}y = \sum_{el}\frac{1}{2C_T}[d]^T[C_T][d] \tag{34}$$

As a result, the mode shape parameter can be obtained by using the above relations without requiring any additional algorithm.

8. Numerical Example 1

In order to check the accuracy of this method; a plate on a two-parameter foundation is considered. This plate problem was solved by Vallabhan et al. (1991), for a uniformly distributed (Fig. 6(a)) and a concentrated (Fig. 6(b)) load, for various depths of soil stratum by using the finite difference method. The same problem is analyzed by using the presented method and the displacements, soil coefficients, mode shape parameters and the bending moments are obtained and presented in Tables 1 and 2.

The elastic constants of the soil: $E_s = 68{,}950$ kN/m^2, $v_s = 0.25$.
The elastic constants of the plate: $E_p = 20{,}685{,}000$ kN/m^2, $v_p = 0.20$.

The thickness of the plate is 0.1524 m, the dimensions are (9.144×12.192 m).

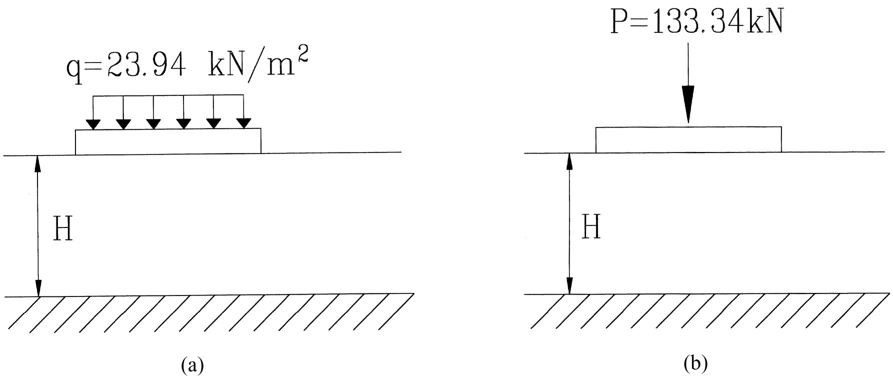

Fig. 6. (a) Uniformly distributed load, (b) concentrated load.

Table 1
The uniformly distributed load

H (m)	Ref.	C (kN/m^3)	C_T (kN/m)	γ	$\mathbf{v}$ (cm)	M_x (kN m/m)
3.048	V.S.D.	27,206	13,452	0.5724	0.0872	0.0529
	P. study	27,192	13,413	0.5766	0.0853	0.0445
6.096	V.S.D.	13,757	25,141	0.9297	0.1524	0.3113
	P. study	13,757	25,205	0.9194	0.1526	0.2880
9.144	V.S.D.	9430	34,753	1.2644	0.1890	0.4224
	P. study	9377	35,293	1.2064	0.1893	0.4109
15.24	V.S.D.	6366	47,366	1.9419	0.2070	0.4892
	P. study	5964	52,332	1.6193	0.2212	0.4671

Table 2
The concentrated load

H (m)	Ref.	C (kN/m^3)	C_T (kN/m)	γ	$\mathbf{v}$ (cm)	M_x (kN m/m)
3.048	V.S.D.	31,610	9565	1.9018	0.0480	12.544
	P. study	31,898	9456	1.9478	0.0818	15.047
6.096	V.S.D.	23,918	11,959	3.4737	0.0975	12.544
	P. study	24,256	11,798	3.5249	0.0845	14.563
9.144	V.S.D.	23,376	12,193	5.1669	0.0975	12.544
	P. study	23,737	12,017	5.2434	0.0846	14.510
15.24	V.S.D.	23,350	12,205	8.6079	0.0975	12.544
	P. study	23,710	12,030	8.7369	0.0846	14.510

The finite element idealization presented in Fig. 7 is used. Due to the symmetry of the problem, only a quarter of the whole system domain is considered. The full compatible 16 degrees-of-freedom elements are used for the idealization of the plate. Thus, with 42 nodal points each having four nodal degrees-of-freedom and 214 nodal points have one nodal degree-of-freedom, the total number of unknowns considered in the computations are 382.

From the comparisons of Table 1 and 2 one may observe that the results are in agreement with each other. The relative errors on γ are 0.015 at the third step, less than 0.001 at the fourth step for a uniformly distributed load and 0.017 at the sixth step, less than 0.001 at the ninth step for a concentrated load, when the thickness of a compressible layer is 15.24 m. The iteration process on γ converges more rapidly when H decreases, or the bending stiffness of the plate increases.

9. Numerical Example 2

The foundation plate, under a vertical column load, shown in Fig. 8(a), is analyzed for different values of plate thickness and compressible layer thickness of the soil. The effects of the above

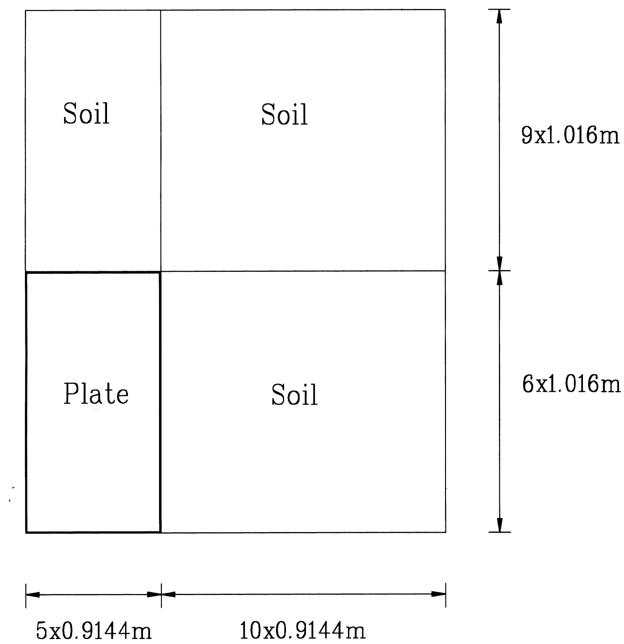

Fig. 7. Finite element idealization.

variables on the mode shape parameter and the soil coefficients are evaluated. The variation of moments at the cross-section are obtained depending on the deflection shape of the plate. The soil finite elements are used in addition to the 16 degrees-of-freedom plate finite element, which includes shear deformations (Çelik, 1996). The width of the soil region is assumed to be greater than the thickness of the compressible layer of the soil. The plate and the soil finite element meshes are shown in Fig. 8(b), where the symmetry condition of the problem is considered.

The elastic constant of the foundation plate: $E_p = 2.10^7$ kN/m^2, $\nu_p = 0.16$.
The elastic constant of the soil: $E_s = 80{,}000$ kN/m^2, $\nu_s = 0.125$.

The values of 'a' which are shown in Fig. 8(b) depending on the thickness of the compressible layer of the soil, are given below:

for $H = 5$ m, $a = 0.6$ m
for $H = 10$ m, $a = 0.9$ m
for $H = 20$ m, $a = 1.8$ m

The value of the mode shape parameter and the soil coefficients are shown in Table 3 for different values of plate thickness and the thickness of compressible layers of the soil.

The variation of the vertical displacements and the bending moments are shown for the plate thickness of $h = 0.6$ m along different axes. The foundation plate is solved as a plate settled on the Winkler soil by use of the elastic bedding coefficient, C, found for a layer thickness of 10 m and the results (W) are plotted on the same diagrams.

From the comparison of the results, it can be seen that the settlement and the internal forces distribution in the foundation plate change seriously, by taking into account the shear parameter

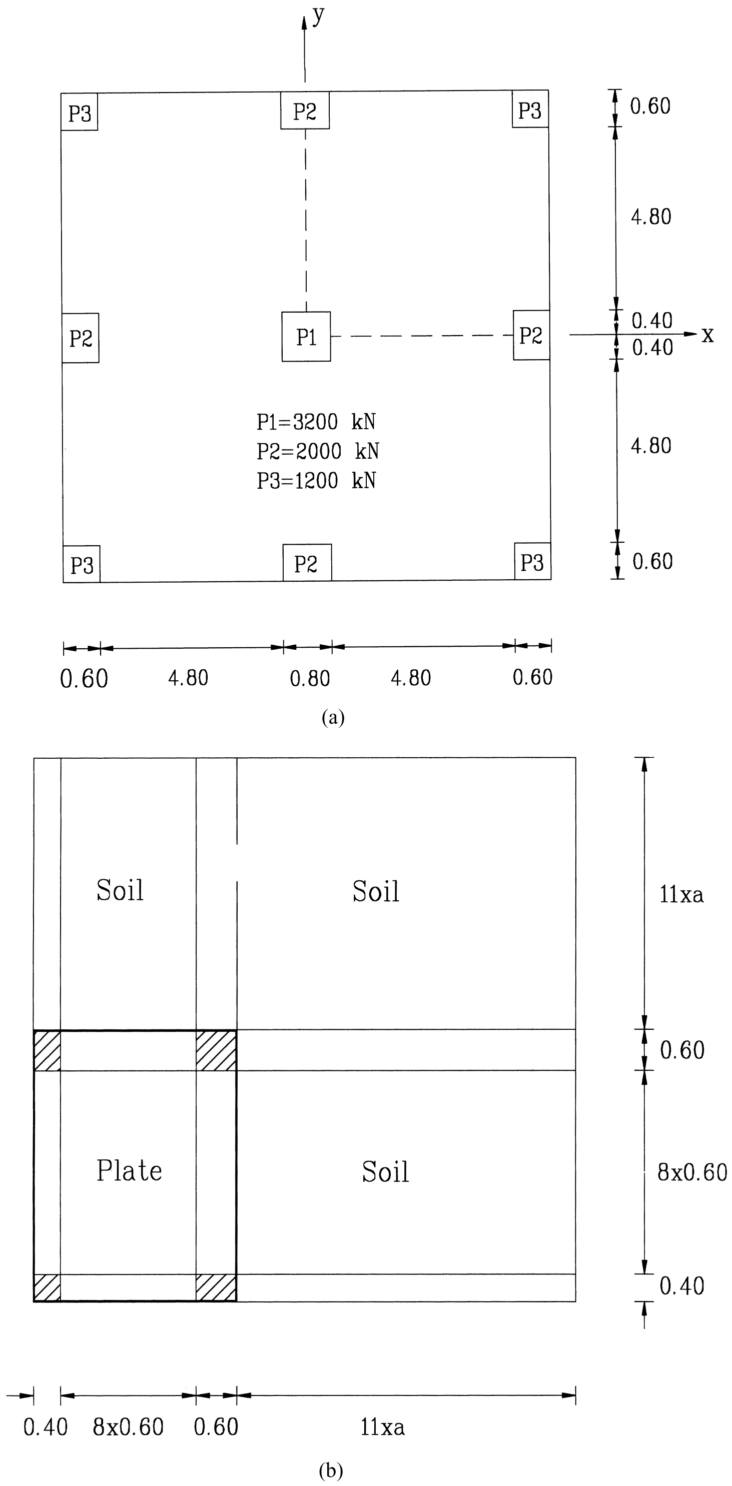

Fig. 8. (a) Foundation plate, (b) finite element idealization.

Table 3

	$h = 0.6$ m			$h = 0.8$ m		
H (m)	γ	C (kN/m^3)	C_T (kN/m)	γ	C (kN/m^3)	C_T (kN/m)
5	1.118	19,733.44	22,901.50	1.001	19,557.70	23,552.10
10	1.327	10,087.80	43,348.10	1.256	10,002.31	44,202.00
20	1.894	5572.80	73,214.50	1.821	5484.70	74,928.20

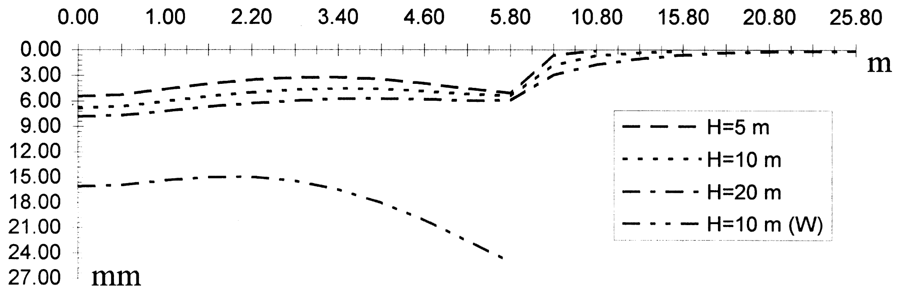

Fig. 9. Vertical displacements (along $x = 5.8$ m axis).

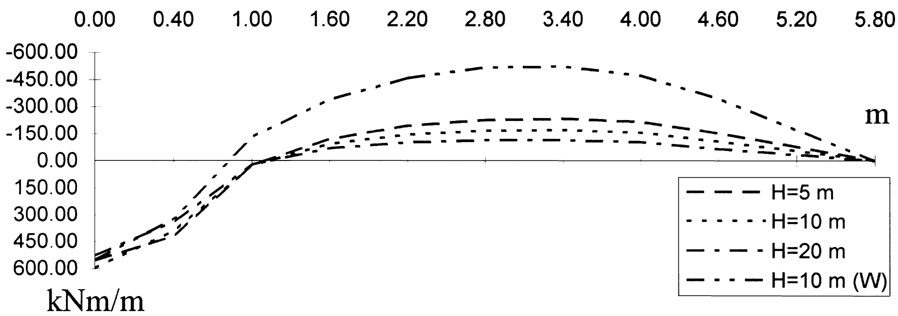

Fig. 10. Bending moment M_y (along $x = 5.8$ m axis).

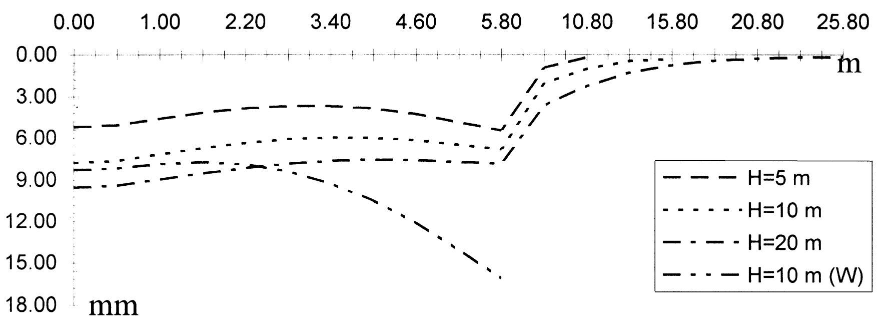

Fig. 11. Vertical displacements (along $x = 0.0$ m axis).

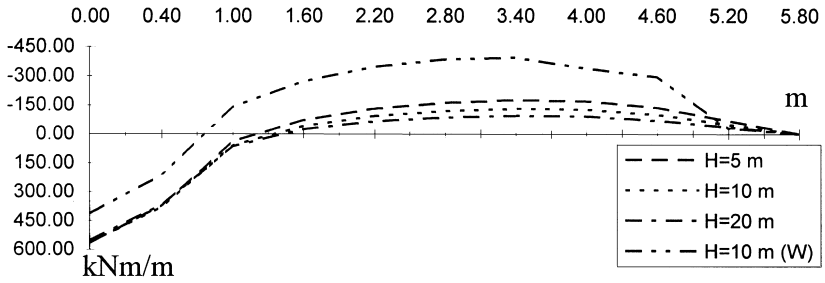

Fig. 12. Bending moment M_y (along $x = 0.0$ m axis).

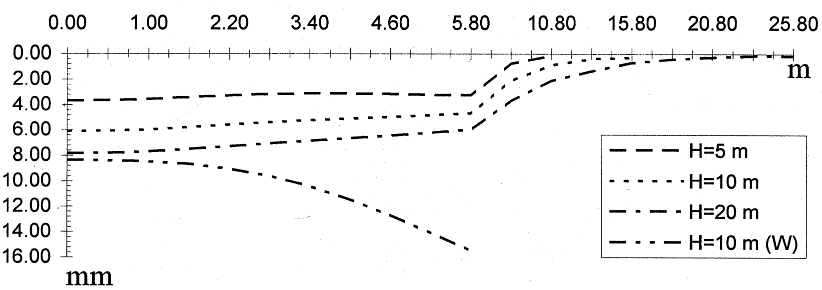

Fig. 13. Vertical displacements (along $x = 2.8$ m axis).

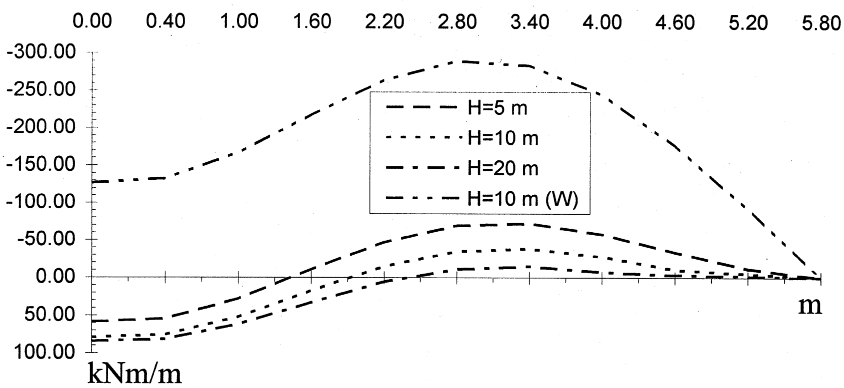

Fig. 14. Bending moment M_y (along $x = 2.8$ m axis).

according to the Winkler assumption and also it is observed that the settlement and soil stress accumulation under the loads on the boundaries and on the corners are decreased. Besides that the decreasing of the side span bending moments and a small increase of the bending moments under concentrated loads are also noticed.

10. Numerical Example 3

The interaction between plates which are close to each other, can change the soil coefficients as well as the internal moments which depend on the deflection shape of the plate. For this reason, as it is seen in Fig. 15(a) the two foundation plates, both similar to the ones considered in Example

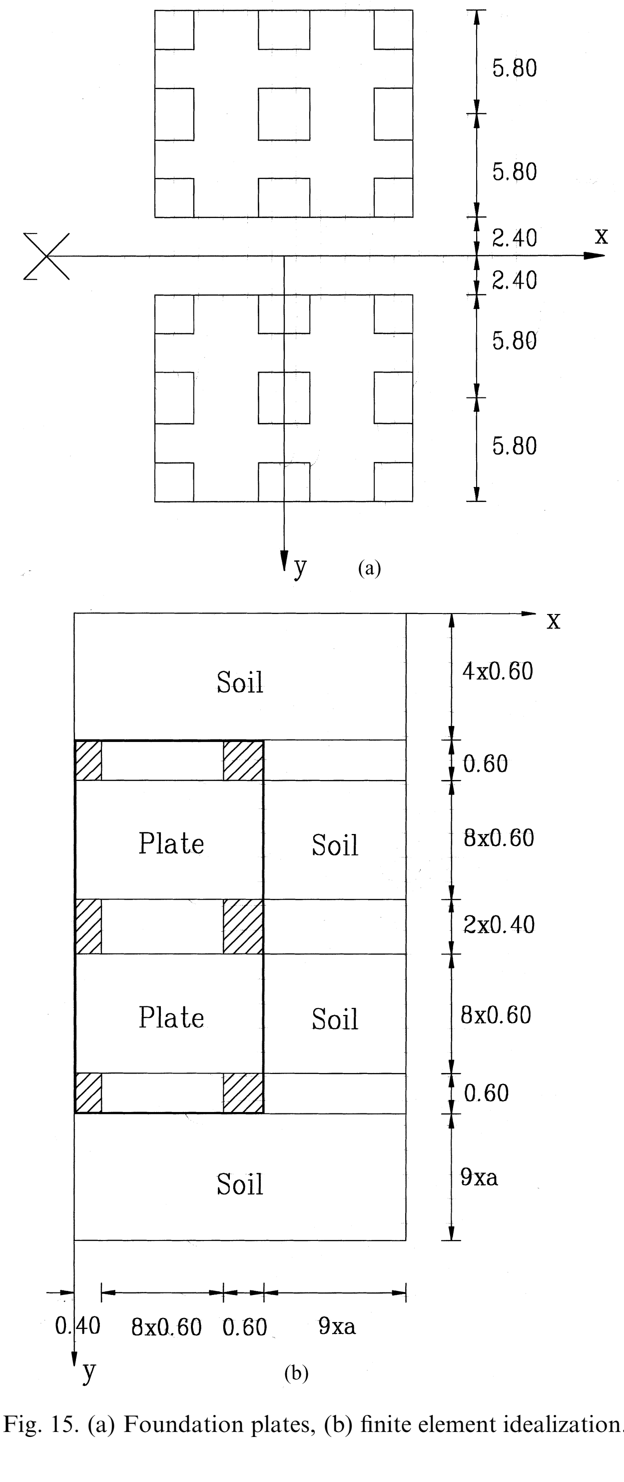

Fig. 15. (a) Foundation plates, (b) finite element idealization.

Table 4

	$h = 0.6$ m			$h = 0.8$ m		
H (m)	γ	C (kN/m^3)	C_T (kN/m)	γ	C (kN/m^3)	C_T (kN/m)
5	1.066	19,650.30	23,191.60	0.950	19,495.00	23,826.80
10	1.160	9904.00	45,324.60	1.089	9842.60	46,133.20
20	1.514	5179.50	82,225.10	1.454	5132.05	83,661.50

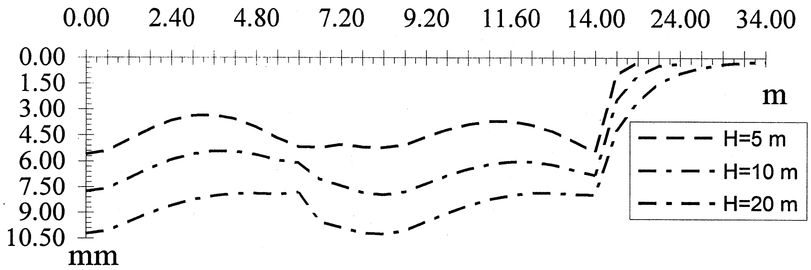

Fig. 16. Vertical displacements (along $y = 2.4$ m axis).

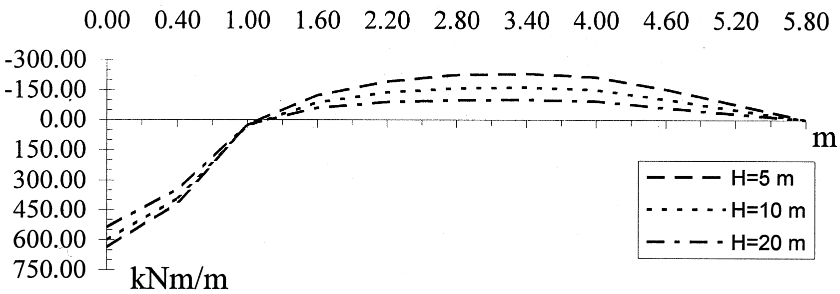

Fig. 17. Bending moments M_x (along $y = 2.4$ m axis).

2 are spaced 4.8 m apart. The mode shape parameter and the soil coefficients are obtained and given in Table 4. The finite element meshes are shown in Fig. 15(b) by using the symmetry condition of the plate geometry.

It is seen that in Tables 3 and 4 the mode shape parameter and the elastic bedding coefficient increase and the shear parameter coefficient decreases as compared to the single foundation plate. Also the vertical displacements and the bending moments are shown for the plate thickness of $h = 0.6$ m along the different axes.

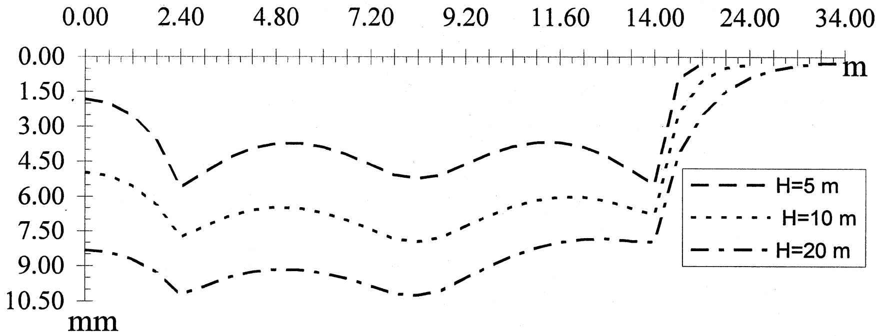

Fig. 18. Vertical displacements (along $x = 0.0$ m axis).

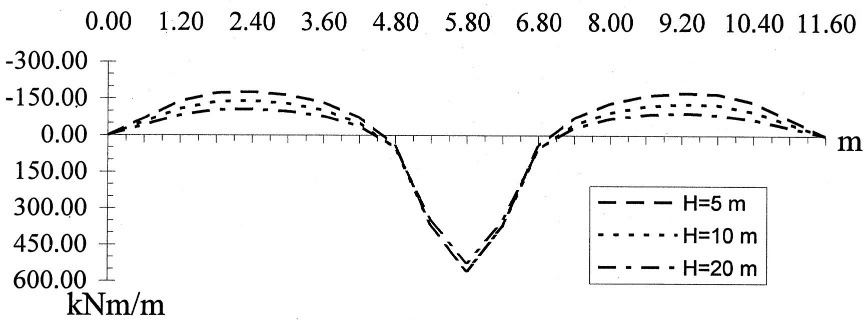

Fig. 19. Bending moments M_y (along $x = 0.0$ m axis).

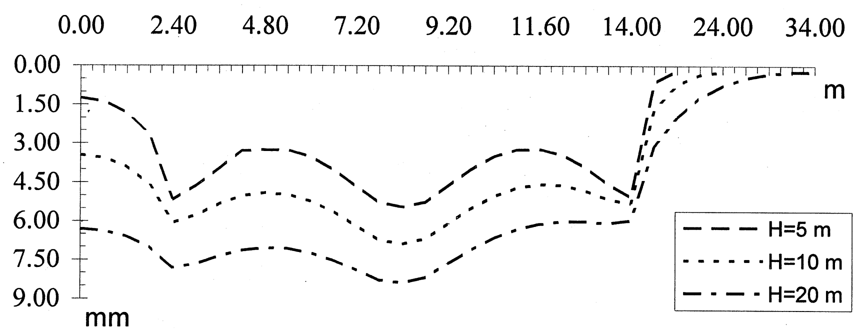

Fig. 20. Vertical displacements (along $x = 5.8$ m axis).

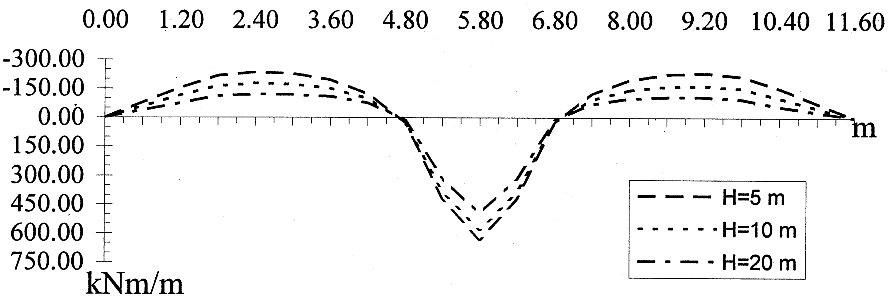

Fig. 21. Bending moments M_y (along $x = 5.8$ m axis).

From the comparison of the results obtained from the second and the third examples it is observed that, when the distance between the foundations are getting smaller than the thickness of the compressible foundation layer, the interaction becomes important and the vertical displacement increases, however, the transverse shear force decreases around the close boundaries. Whereas, when the distance between the foundations gets bigger than the thickness of the compressible foundation layer, the interaction becomes negligible.

11. Conclusion

In this study an iterative method is developed in order to analyze the plate on the two-parameter foundation where the soil finite elements are used in addition to the plate finite elements, so that the displacements for the plate–soil system, the bending and the twisting moments for the plate and the shear stresses of the soil can be computed. Also the elastic bedding coefficients and the shear parameter coefficients can be obtained by using the elastic constants, the thickness of the compressible layer and the mode shape parameter. Due to the character of the problem, the mode shape parameter depends on the dimensions of the plate load case and the mode shape of the soil surface. Further numerical results can be found in Çelik (1996), where the extension of the presented method to circular plates on a two-parameter elastic foundation is also developed. The extension of the model to include buckling and vibration of the plate on the elastic foundation is also possible.

Appendix 1: Elastic bedding and shear parameter matrices of a fully compatible plate finite element

The numbering and sign convention of the nodal displacements are shown in Fig. 22. The elastic bedding and shear parameter matrices can be partitioned into submatrices, which have dimensions of 4×4

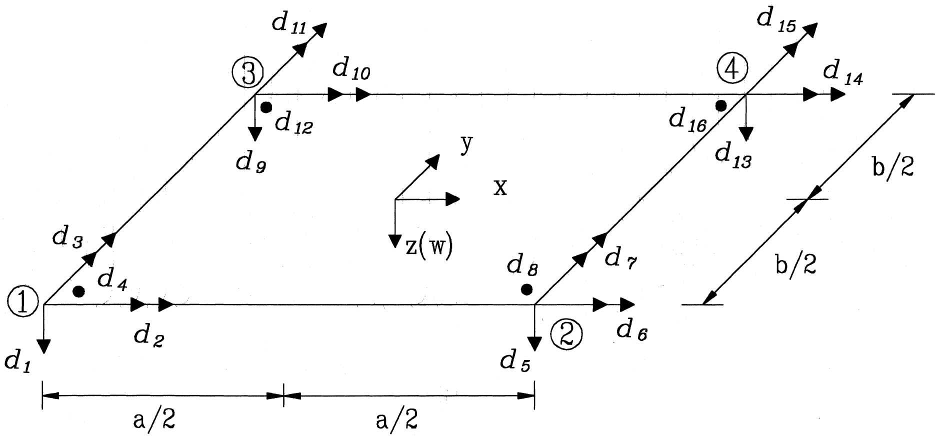

Fig. 22. 16 degrees-of-freedom plate element.

$$[C] = \begin{bmatrix} [C]_{11} & [C]_{12} & [C]_{13} & [C]_{14} \\ [C]_{21} & [C]_{22} & [C]_{23} & [C]_{24} \\ [C]_{31} & [C]_{32} & [C]_{33} & [C]_{34} \\ [C]_{41} & [C]_{42} & [C]_{43} & [C]_{44} \end{bmatrix} \quad [C_{\mathrm{T}}] = \begin{bmatrix} [C_{\mathrm{T}}]_{11} & [C_{\mathrm{T}}]_{12} & [C_{\mathrm{T}}]_{13} & [C_{\mathrm{T}}]_{14} \\ [C_{\mathrm{T}}]_{21} & [C_{\mathrm{T}}]_{22} & [C_{\mathrm{T}}]_{23} & [C_{\mathrm{T}}]_{24} \\ [C_{\mathrm{T}}]_{31} & [C_{\mathrm{T}}]_{32} & [C_{\mathrm{T}}]_{33} & [C_{\mathrm{T}}]_{34} \\ [C_{\mathrm{T}}]_{41} & [C_{\mathrm{T}}]_{42} & [C_{\mathrm{T}}]_{43} & [C_{\mathrm{T}}]_{44} \end{bmatrix} \tag{35}$$

where the matrices $[C]_{ij}$ and $[C_{\mathrm{T}}]_{ij}$ represent the nodal forces at i nodal point due to the unit displacements at j nodal point. From Betty's law, it follows:

$$[C]_{ii}^{T} = [C]_{ii}, \quad [C]_{ij}^{T} = [C]_{ji} \quad \text{and} \quad [C_{\mathrm{T}}]_{ii}^{T} = [C_{\mathrm{T}}]_{ii}, \quad [C_{\mathrm{T}}]_{ij}^{T} = [C_{\mathrm{T}}]_{ji} \tag{36}$$

Also by the use of symmetry of the rectangular plate and considering that the nodal forces due to symmetric displacements are symmetric, it yields:

$$\begin{aligned} &[C]_{22} = [T_y][C]_{11}[T_y] \quad [C_{\mathrm{T}}]_{22} = [T_y[C_{\mathrm{T}}]_{11}[T_y] \\ &[C]_{23} = [T_y][C]_{14}[T_y] \quad [C_{\mathrm{T}}]_{23} = [T_y][C_{\mathrm{T}}]_{14}[T_y] \\ &[C]_{24} = [T_y][C]_{13}[T_y] \quad [C_{\mathrm{T}}]_{24} = [T_y][C_{\mathrm{T}}]_{13}[T_y] \\ &[C]_{33} = [T_x][C]_{11}[T_x] \quad [C_{\mathrm{T}}]_{33} = [T_x][C_{\mathrm{T}}]_{11}[T_x] \\ &[C]_{34} = [T_x][C]_{12}[T_x] \quad [C_{\mathrm{T}}]_{34} = [T_x][C_{\mathrm{T}}]_{12}[T_x] \\ &[C]_{44} = [T_y][T_x][C]_{11}[T_x][T_y] \quad [C_{\mathrm{T}}]_{44} = [T_y][T_x][C_{\mathrm{T}}]_{11}[T_x][T_y] \end{aligned} \tag{37}$$

where $[T_x]$ and $[T_y]$ are diagonal transformation matrices given below:

$$[T_x] = \begin{bmatrix} 1 & 0 & 0 & 0 \\ 0 & -1 & 0 & 0 \\ 0 & 0 & 1 & 0 \\ 0 & 0 & 0 & -1 \end{bmatrix} \quad [T_y] = \begin{bmatrix} 1 & 0 & 0 & 0 \\ 0 & 1 & 0 & 0 \\ 0 & 0 & -1 & 0 \\ 0 & 0 & 0 & -1 \end{bmatrix} \tag{38}$$

From the above relations, the complete elastic bedding and the shear parameter matrices can be obtained from the submatrices $[C]_{11}$, $[C]_{12}$, $[C]_{13}$ and $[C]_{14}$, $[C_T]_{11}$, $[C_T]_{12}$, $[C_T]_{13}$ and $[C_T]_{14}$. These matrices are given as follows:

Elastic bedding submatrix of a full compatible finite element

$$[C]_{11} = \frac{Cab}{1225} \begin{bmatrix} 169 & -\frac{143}{6}b & \frac{143}{6}a & \frac{121}{36}ab \\ -\frac{143}{6}b & \frac{13}{3}b^2 & -\frac{121}{36}ab & -\frac{22}{36}ab^2 \\ \frac{143}{6}a & -\frac{121}{36}ab & \frac{13}{3}a^2 & \frac{22}{36}ab \\ \frac{121}{36}ab & -\frac{22}{36}ab^2 & \frac{22}{36}ab & \frac{a^2b^2}{9} \end{bmatrix}$$

$$[C]_{12} = \frac{Cab}{1225} \begin{bmatrix} 58.5 & -\frac{33}{4}b & -\frac{169}{12}a & -\frac{143}{72}ab \\ -\frac{33}{4}b & 1.5b^2 & \frac{143}{72}ab & \frac{13}{36}ab^2 \\ \frac{169}{12}a & -\frac{143}{72}ab & \frac{13}{4}a^2 & -\frac{11}{24}a^2b \\ \frac{143}{72}ab & -\frac{13}{36}ab^2 & -\frac{11}{24}a^2b & \frac{a^2b^2}{12} \end{bmatrix}$$

$$[C]_{13} = \frac{Cab}{1225} \begin{bmatrix} 58.5 & \frac{42.25a}{3} & 8.25a & -\frac{71.5ab}{36} \\ -\frac{42.25b}{3} & -3.25b^2 & -\frac{71.5ab}{36} & \frac{16.5ab^2}{36} \\ 8.25a & \frac{71.5ab}{36} & 1.5a^2 & -\frac{13a^2b}{36} \\ \frac{71.5ab}{36} & \frac{16.5ab^2}{36} & \frac{13a^2b}{36} & -\frac{0.75a^2b^2}{9} \end{bmatrix}$$

$$[C]_{14} = \frac{Cab}{1225}\begin{bmatrix} 20.25 & 4.875b & -4.875a & \frac{42.25ab}{36} \\ -4.875b & -1.125b^2 & \frac{42.25ab}{36} & -\frac{9.75ab^2}{36} \\ 4.875a & \frac{42.25ab}{36} & -1.125a^2 & \frac{9.75a^2b}{36} \\ \frac{42.25ab}{36} & \frac{9.75ab^2}{36} & -\frac{9.75a^2b}{36} & \frac{2.25a^2b^2}{36} \end{bmatrix}$$

Shear parameter submatrix of a full compatible element

$$[C_T]_{11} = \frac{2C_T}{350}\begin{bmatrix} 156(\alpha+\beta) & -(22\beta+13\alpha)b & (22\alpha+13\beta)a & \frac{11}{6}(\alpha+\beta)ab \\ & \left(4\beta+\frac{52}{3}\alpha\right)b^2 & -\frac{11}{6}(\alpha+\beta)ab & -\left(\frac{\beta}{3}+\frac{22}{9}\alpha\right)ab^2 \\ & & \left(4\alpha+\frac{52}{3}\beta\right)a^2 & \left(\frac{\alpha}{3}+\frac{22}{9}\beta\right)a^2b \\ \text{symmetric} & & & \frac{4}{9}(\alpha+\beta)a^2b^2 \end{bmatrix}$$

$$[C_T]_{12} = \frac{2C_T}{350}\begin{bmatrix} 54\alpha-156\beta & (22\beta-4.5\alpha)b & -13(\alpha-\beta)a & \left(\frac{11}{6}\beta-\frac{13}{12}\alpha\right)ab \\ (22\beta-4.5\alpha)b & -(4\beta-6\alpha)b^2 & \left(-\frac{11}{6}\beta+\frac{13}{12}\alpha\right)ab & -\left(\frac{\beta}{3}-\frac{13}{9}\alpha\right)ab^2 \\ 13(\alpha-\beta)a & \left(\frac{11}{6}\beta-\frac{13}{12}\alpha\right)ab & -\left(3\alpha+\frac{13}{3}\beta\right)a^2 & -\left(\frac{\alpha}{4}+\frac{11}{18}\beta\right)a^2b \\ -\left(\frac{11}{6}\beta-\frac{13}{12}\alpha\right)ab & \left(\frac{\beta}{3}-\frac{13}{9}\alpha\right)ab^2 & -\left(\frac{\alpha}{4}+\frac{11}{18}\beta\right)a^2b & -\left(\frac{\beta}{9}+\frac{\alpha}{3}\right)a^2b^2 \end{bmatrix}$$

$$[C_T]_{13} = \frac{2C_T}{350}\begin{bmatrix} 54\beta-156\alpha & 13(\beta-\alpha)b & -(22\alpha-4.5\beta)a & \left(\frac{11}{6}\alpha-\frac{13}{12}\beta\right)ab \\ 13(\alpha-\beta)b & -\left(3\beta+\frac{13}{3}\alpha\right)b^2 & \left(\frac{11}{6}\alpha-\frac{13}{12}\beta\right)ab & \left(\frac{\beta}{4}+\frac{11}{18}\alpha\right)ab^2 \\ -(22\alpha-4.5\beta)a & -\left(\frac{11}{6}\alpha+\frac{13}{12}\beta\right)ab & -(4\alpha-6\beta)a^2 & \left(\frac{\alpha}{3}-\frac{13}{9}\beta\right)a^2b \\ -\left(\frac{11}{6}\alpha-\frac{13}{12}\beta\right)ab & \left(\frac{\beta}{4}+\frac{11}{18}\alpha\right)ab^2 & -\left(\frac{\alpha}{3}-\frac{13}{9}\beta\right)a^2b & -\left(\frac{\beta}{3}+\frac{\alpha}{9}\right)a^2b^2 \end{bmatrix}$$

$$[C_T]_{14} = \frac{2C_T}{350}\begin{bmatrix} -54(\alpha+\beta) & -(13\beta+4.5\alpha)b & (13\alpha+4.5\beta)a & -\frac{13}{12}(\alpha+\beta)ab \\ (13\beta+4.5\alpha)b & (3\beta-1.5\alpha)b^2 & -\frac{13}{12}(\alpha+\beta)ab & \left(\frac{\beta}{4}-\frac{13}{36}\alpha\right)ab^2 \\ -(13\alpha+4.5\beta)a & -\frac{13}{12}(\alpha+\beta)ab & (3\alpha-1.5\beta)a^2 & -\left(\frac{\alpha}{4}-\frac{13}{36}\beta\right)a^2b \\ -\frac{13}{12}(\alpha+\beta)ab & -\left(\frac{\beta}{4}-\frac{13}{36}\alpha\right)ab^2 & \left(\frac{\alpha}{4}-\frac{13}{36}\beta\right)a^2b & \frac{1}{12}(\alpha+\beta)a^2b^2 \end{bmatrix}$$

Appendix 2: Elastic bedding and shear parameter matrices of a plate finite element having 12 degrees-of-freedom

The numbering and sign convention of nodal displacements are shown in Fig. 23. The elastic bedding and shear parameter matrices can be partitioned into submatrices, which have dimension of 3×3 as (34).

The equalities (36) and (37) of Appendix 1 remain entirely valid where the diagonal transformation matrices must be changed as;

$$[T_x] = \begin{bmatrix} 1 & 0 & 0 \\ 0 & -1 & 0 \\ 0 & 0 & 1 \end{bmatrix} \quad [T_y] = \begin{bmatrix} 1 & 0 & 0 \\ 0 & 1 & 0 \\ 0 & 0 & -1 \end{bmatrix} \tag{39}$$

Thus, the complete elastic bedding and the shear parameter matrices can be obtained from the submatrices $[C]_{11}$, $[C]_{12}$, $[C]_{13}$ and $[C]_{14}$, $[C_T]_{11}$, $[C_T]_{12}$, $[C_T]_{13}$ and $[C_T]_{14}$. These matrices are given as follows:

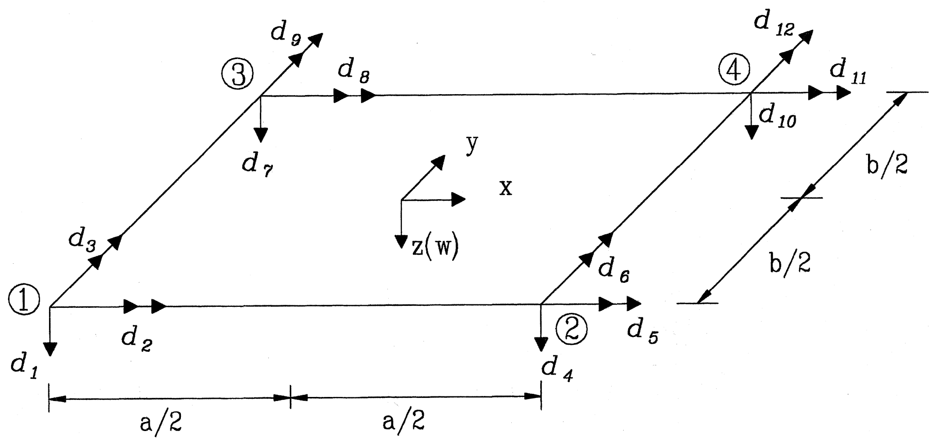

Fig. 23. 12 degrees-of-freedom plate element.

Elastic bedding submatrix of a finite element having 12 degrees-of-freedom

$$[C]_{11} = \frac{Cab}{25{,}200}\begin{bmatrix} 3454 & -461b & 461a \\ & 80b^2 & -63ab \\ \text{symmetric} & & 80a^2 \end{bmatrix}$$

$$[C]_{12} = \frac{Cab}{25{,}200}\begin{bmatrix} 1226 & -199b & -274a \\ -199b & 40b^2 & 42ab \\ 274a & -42ab & -60a^2 \end{bmatrix}$$

$$[C]_{13} = \frac{Cab}{25{,}200}\begin{bmatrix} 1226 & 274b & 199a \\ -274b & -60b^2 & -42ab \\ 199a & 42ab & 40a^2 \end{bmatrix}$$

$$[C]_{14} = \frac{Cab}{25{,}200}\begin{bmatrix} 394 & 116b & -116a \\ -116b & -30b^2 & 28ab \\ 116a & 28ab & -30a^2 \end{bmatrix}$$

Shear parameter submatrix of an element having 12 degrees-of-freedom

$$[C_{\mathrm{T}}]_{11} = \frac{2C_{\mathrm{T}}}{210}\begin{bmatrix} 92(\alpha+\beta) & -(11\beta+7\alpha)b & (11\beta+7\alpha)a \\ & (-2\beta+\frac{28}{3}\alpha)b^2 & 0 \\ \text{symmetric} & 0 & (2\alpha^2+\frac{28}{3}\beta)a^2 \end{bmatrix}$$

$$[C_{\mathrm{T}}]_{12} = \frac{2C_{\mathrm{T}}}{210}\begin{bmatrix} 34\alpha-92\beta & (11\beta-3.5\alpha)b & -(6.5\alpha-7\beta)a \\ (11\beta-3.5\alpha)b & (-2\beta+\frac{14}{3}\alpha)b^2 & 0 \\ (6.5\alpha-7\beta)a & 0 & -(1.5\alpha^2+\frac{7}{3})a^2 \end{bmatrix}$$

$$[C_{\mathrm{T}}]_{13} = \frac{2C_{\mathrm{T}}}{210}\begin{bmatrix} -92\alpha+34\beta & (6.5\beta-7\alpha)b & -(115\alpha-3.5\beta)a \\ -(6.5\beta-7\alpha)b & -(1.5\beta+\frac{7}{3}\alpha)b^2 & 0 \\ -(115\alpha-3.5\beta)a & 0 & (-2\alpha+\frac{14}{3}\beta)a^2 \end{bmatrix}$$

$$[C_{\mathrm{T}}]_{14} = \frac{2C_{\mathrm{T}}}{210}\begin{bmatrix} -34(\alpha+\beta) & -(6.5\beta+3.5\alpha)b & (6.5\alpha+3.5\beta)a \\ (6.5\beta+3.5\alpha)b & (1.5\beta-\frac{7}{6}\alpha)b^2 & 0 \\ -(6.5\alpha+3.5\beta)a & 0 & (1.5\alpha^2-\frac{7}{6}\beta)a^2 \end{bmatrix}$$

References

Adini, A., Clough, R.W., 1960. Analysis of plate bending by the finite element method. National Science Foundation (Grant G 7337), Washington, DC., submitted.

Bogner, F.K., Fox, R.L., Schmit, L.A., 1966. The generation of interelement-compatible stiffness and mass matrices by the use of interpolation formulas. Proceedings of the Conference on Matrix in Structural Mechanics. Air Force Institute of Technology, Wright Patterson Air Force Base, Ohio.

Çelik, M., 1996. Plate finite element formulation including shear deformation and a method for the analysis of plate on two-parameter foundations. Ph.D. thesis, Technical University of Istanbul (in Turkish).

Eisenberger, M., Bielak, J. 1992. Finite beams on infinite two-parameter elastic foundation. Computers and Structures 42, 661–664.

Jones, R., Xenophontos, J., 1977. The Vlasov foundation model. Int. J. Mech. Sci. 19, 317–323.

Karamanlidis, D., Prakash, V., 1988. Buckling and vibration analysis of flexible beams resting on an elastic half-space. Earthquake Engineering and Structural Dynamics 16, 1103–1114.

Nogami, T., Lam, Y.C., 1987. Two-parameter layer model for analysis of slabs on elastic foundations. Journal of Engineering Mechanics 113 (9), 1279–1291.

Nogami, T., O'Neil, M.W., 1985. Beam on generalized two-parameter foundation. Journal of Engineering Mechanics 111 (5), 664–679.

Razaqpur, A.G., Shah, K.R., 1991. Exact analysis of beams on two parameter elastic foundations. International Journal of Solids and Structures 27 (4), 435–454.

Vallabhan, C.V., Daloğlu, A.T., 1997. Consistent FEM-Vlasov model for slabs on elastic foundations. Seventh International Conference on Computing in Civil and Building Engineering, 19–21 August, Seoul, Korea, pp. 57–62.

Vallabhan, C.V.G., Das, Y.C., 1988. Parametric study of beams on elastic foundations. Journal of Engineering Mechanics 114 (14), 2072–2082.

Vallabhan, C.V., Das, Y.C., 1991. A refined model for beams on elastic foundations. International Journal of Solids and Structures 27 (5), 629–637.

Vallabhan, C.V., Das, Y.C. 1991. Analysis of circular tank foundations. Journal of Engineering Mechanics 117 (4), 789–797.

Vallabhan, C.V.G., Straughan, W.T., Das, Y.C., 1991. Refined model for analysis of plates on elastic foundation. Journal of Engineering Mechanic 117 (12), 2830–2844.

Vlasov, V.Z., Leont'ev, U.N., 1966. Beams, Plates and Shells on Elastic Foundation. Israel Program for Scientific Translation, Jerusalem.